APPLIED AND ENVIRONMENTAL MICROBIOLOGY, Sept. 2000, p. 4058–4067 Vol. 66, No. 9
0099-2240/00/$04.00+0

Flexible Community Structure Correlates with Stable Community Function in Methanogenic Bioreactor Communities Perturbed by Glucose

ANA S. FERNANDEZ,[1,2]† SYED A. HASHSHAM,[1,3] SHERRY L. DOLLHOPF,[1,4] LUTGARDE RASKIN,[5] OLGA GLAGOLEVA,[1,4] FRANK B. DAZZO,[1,4] ROBERT F. HICKEY,[1,3,6] CRAIG S. CRIDDLE,[1,3]‡ AND JAMES M. TIEDJE[1,4]*

Center for Microbial Ecology,[1] Department of Civil and Environmental Engineering,[3] and Department of Microbiology,[4] Michigan State University, East Lansing, Michigan 48824; Cátedra de Microbiología, Facultad de Química, Montevideo, Uruguay[2]; Department of Civil Engineering, Newmark Civil Engineering Laboratory, University of Illinois at Urbana-Champaign, Urbana, Illinois, 61801[5]; and EFX Systems, Lansing, Michigan 48910[6]

Received 1 February 2000/Accepted 29 May 2000

Methanogenic bioreactor communities were used as model ecosystems to evaluate the relationship between functional stability and community structure. Replicated methanogenic bioreactor communities with two different community structures were established. The effect of a substrate loading shock on population dynamics in each microbial community was examined by using morphological analysis, small-subunit (SSU) rRNA oligonucleotide probes, amplified ribosomal DNA (rDNA) restriction analysis (ARDRA), and partial sequencing of SSU rDNA clones. One set of replicated communities, designated the high-spirochete (HS) set, was characterized by good replicability, a high proportion of spiral and short thin rod morphotypes, a dominance of spirochete-related SSU rDNA genes, and a high percentage of *Methanosarcina*-related SSU rRNA. The second set of communities, designated the low-spirochete (LS) set, was characterized by incomplete replicability, higher morphotype diversity dominated by cocci, a predominance of *Streptococcus*-related and deeply branching *Spirochaetales*-related SSU rDNA genes, and a high percentage of *Methanosaeta*-related SSU rRNA. In the HS communities, glucose perturbation caused a dramatic shift in the relative abundance of fermentative bacteria, with temporary displacement of spirochete-related ribotypes by *Eubacterium*-related ribotypes, followed by a return to the preperturbation community structure. The LS communities were less perturbed, with *Streptococcus*-related organisms remaining prevalent after the glucose shock, although changes in the relative abundance of minor members were detected by morphotype analysis. A companion paper demonstrates that the more stable LS communities were less functionally stable than the HS communities (S. A. Hashsham, A. S. Fernandez, S. L. Dollhopf, F. B. Dazzo, R. F. Hickey, J. M. Tiedje, and C. S. Criddle, Appl. Environ. Microbiol. 66:4050–4057, 2000).

Design and operation of bioreactors for waste management are an exercise in ecosystem management. Bioreactor communities contain dozens of interacting microbial populations, even when a single substrate is provided. Improved design and management of such communities depend upon the formulation of experimentally validated ecological concepts. Not surprisingly, much of the engineering design of complex bioreactors has been empirical, and low applied organic loading rates and long residence times have been used to avoid failure (27). More fundamental approaches group populations with similar functions into guilds. Ecological models are formulated by assigning kinetic parameters to each guild and defining the electron and energy flow between the guilds. Such models are useful for design and simulation under normal operating conditions, but their utility for fluctuating conditions is less clear (14). Competition among species for substrates, acid tolerance, syntrophic interactions, and other physiological properties of bacterial populations that lead to rapid changes in bacterial community composition control the reactions of bioreactors to fluctuating conditions. Some models that try to account for these dynamics have been proposed (14, 15, 24), but there is uncertainty in these models because of the presence of minority community members that may become dominant when operational parameters change.

Recently developed molecular techniques in microbial ecology provide an opportunity to link the microbial community structure to the functional attributes of wastewater treatment, making the formulation of more sophisticated models feasible (1, 13). Many previous studies of anaerobic bioreactor communities have used small-subunit (SSU) rRNA probes to investigate competition between methanogens and sulfidogens, the role of sulfate-reducing bacteria (SRB) as syntrophic organisms, and the effects of substrate composition and mixing regimes on various syntrophic and methanogenic populations (9, 19, 20). Robust tools of computer-assisted microscopy and image analysis have also been developed recently, making it possible to rapidly analyze the morphological diversity of complex microbial communities at frequent sampling points and thereby detect dynamic shifts in community structure with high sensitivity, precision, and accuracy (12; http://macorb.uthscsa.edu/dig/itdesc.html). This paper focuses on the ecological

* Corresponding author. Mailing address: Center for Microbial Ecology, Michigan State University, 540 Plant and Soil Science Building, E. Lansing, MI 48824. Phone: (517) 353-9021. Fax: (517) 353-2917. E-mail: tiedjej@msu.edu.

† Present address: Cátedra de Microbiología, Facultad de Química, Montevideo, Uruguay.

‡ Present address: Department of Civil and Environmental Engineering, Stanford University, Stanford, CA 94305.

shifts in the community structure of glucose-fed methanogenic bioreactor communities following the application of a large substrate shock load. We used several complimentary methods to dissect and compare these communities before the perturbation, and we present a conceptual model of community structure for each. We also describe changes in community structure following the glucose shock and contrast the types of community shifts observed. A companion paper describes the functional response of these same communities and demonstrates that they metabolized glucose by different pathways. One set of communities metabolized glucose by several pathways operating in parallel (glucose to acetate, glucose to butyrate, etc.) and exhibited rapid recovery to preperturbation conditions. A second set of communities processed glucose in a serial manner (glucose to lactate to butyrate to acetate) and recovered much more slowly to preperturbation conditions (11). Paradoxically, communities with a more stable community structure were less stable functionally, suggesting that an inflexible community structure may be associated with greater functional instability.

MATERIALS AND METHODS

Bioreactor design, operation, and replication. Eight continuously stirred methanogenic bioreactors were operated at 35°C with a 16-day residence time and received 12.5 ml of a buffered glucose solution (44.4 mM glucose, 83.3 mM $NaHCO_3$) per day plus 5 ml of 40×-diluted nutrient solution (11) per day. Four reactors (designated the high-spirochete [HS] set) were inoculated with fluid from a 16-liter methanogenic bioreactor that had operated for 200 days with glucose as the sole carbon and energy source. The other four reactors (designated the low-spirochete [LS] set) were inoculated with fluid from a different methanogenic bioreactor that had been supplied with glucose for 60 days. The HS and LS sets were operated at steady-state conditions for 80 and 32 days, respectively, during which time the concentrations of glucose in the reactors were below the detection limit of the high-performance liquid chromatography methods used (11). On day 0 both sets were perturbed with a shock load of glucose by instantaneously increasing the concentration of glucose in the reactor liquid to approximately 38 mM using a concentrated sterile stock solution that also contained a 50:50 mixture of $NaHCO_3$ and $KHCO_3$ in order to provide buffer for the additional organic acids expected from glucose.

Morphological analysis. Bioreactor community samples were immobilized on agarose-coated slides, examined by phase-contrast microscopy, and analyzed by computer-assisted digital morphological analysis. Coated slides were prepared as described by Pfennig and Wagener (16) except that washed and autoclaved Boehringer Mannheim LE agarose (1.6%, wt/vol) was used instead of agar. Freshly collected samples were dispersed by multiple, rapid passages through a 25-gauge needle and then diluted to slight turbidity to achieve an ideal spatial density of separated cells (ca. 100 cells per micrograph) for morphotype classification. Exactly 26 μl of a diluted cell suspension was placed on an agarose-coated slide. The sample was immediately covered with a glass coverslip (22 by 22 mm; no. 1.5 thickness) and stored in a humid chamber until it was examined. Photomicrographs of refractile, immobilized cells were made by using phase-contrast microscopy and Kodak TMax 100 ASA black and white negative film (final magnification, ×400) with a Zeiss Photomicroscope I equipped with a 100× PlanApochromat phase 3 oil immersion objective, a quartz halogen lamp, and a 546-nm interference contrast filter and alignment with Köhler illumination. Autofluorescent methanogens were examined by epifluorescence microscopy with a Zeiss Axioscope equipped with an HBO 100 illuminator and a 02 filter set (excite G365, beamsplit FT 395, emit LP 420) and were photographed with Kodak TMax 400 ASA film.

For image analysis, the 35-mm micrograph negatives were transilluminated with fiber optics, converted to positive full-frame video images using a DageMTI NC-70 nuvicon camera with a Rodenstock 50-mm lens, and digitized. Classification of operational morphological units (OMUs) was performed at ca. 3,000× by using Bioquant System IV and MegX image analysis software initially (4, 18) and custom CMEIAS plugins (12) operating in UTHSCSA ImageTool Ver. 1.27 software (http://macorb.uthscsa.edu/dig/itdesc.html) later. Bacterial biovolumes were calculated after the mean volume per cell was determined for each different morphotype by using CMEIAS software. Images were spatially calibrated using digital micrographs of a 2.00-mm by 10.0-μm slide micrometer at the same magnification. The data for this study were derived from image analysis of 1,440 photomicrographs, and an average of 1,145 cells were analyzed per sample. Various indices of community structure were calculated from data for OMU richness and equitability of relative abundance using EcoStat software (Trinity Software, Plymouth, N.H.).

Amplified ribosomal DNA restriction analysis (ARDRA). Samples (10 ml) were taken on days 0 and 8 for both reactor sets, on day 16 for the HS reactor set, and on day 24 for one of the HS reactors (reactor 8). DNA extraction, amplification of bacterial SSU ribosomal DNA (rDNA), cloning, and restriction digestion were performed as previously described (6, 13). Each restriction pattern was defined as an operational taxonomic unit (OTU). Clones having the same OTU were grouped, and the frequency of each OTU was calculated. A total of 40 clones were analyzed for every time point for each of the replicate reactors. No common OTUs were found in all eight reactors, and only 7% of all OTUs were shared by HS and LS libraries. Restriction patterns are identified by bioreactor set (using the LS and HS designations) and by the frequency of the OTU in the reactor library, as indicated by a roman numeral (e.g., LS II indicates the second-most-common OTU in the entire LS library).

Sequencing and phylogenetic analysis. Dominant OTUs were partially sequenced (400 bp), and the sequence was analyzed as described previously (6), except that sequence data alignment was performed with the CLUSTAL W software package (28) and was corrected by manual inspection. A phylogenetic tree was constructed by the neighbor-joining method (22) with the PHYLIP 3.5c software package and the Jukes-Cantor distance model (5). Bootstrap resampling analysis for 100 replicates was performed to estimate the confidence of the tree topology (5).

SSU rRNA oligonucleotide probing. Approximately 10-ml samples from reactors 1, 2, 6, and 7 were taken immediately before the glucose pulse and centrifuged for 10 min at 8,000 × *g*. The supernatants were discarded, and the pellets were immediately stored at −80°C until the nucleic acids could be extracted. Phenol-chloroform-isoamyl alcohol (100:24:1 [vol/vol/vol]) extraction was used to extract RNA. The concentration and quality of the extracted rRNA were measured spectrophotometrically at 260 nm and by electrophoresis through a 10% polyacrylamide gel. Quantitative rRNA membrane hybridizations were performed as previously described by Raskin et al. (19). The following reference organisms (and probes) were used: *Desulfovibrio africanus* (S-D-Bact-0338-a-A-18, S-F-Dsv-0687-a-A-16), *Methanosarcina* sp. strain WH2 (S-G-Msar-0821-a-A-24), *Methanobacterium bryantii* M.o.H.G. (= DSM 862) (S-F-Mbac-0310-a-A-22), *Methanosaeta concilli* FE (= DSM 3013) (S-G-Msae-0381-a-A-22), *Syntrophobacter fumaroxidans* MPOB (SYNB838), *Syntrophomonas wolfei* LYB (SYNM700), *Desulfobulbus propionicus* (S-G-Dsbb-0660-a-A-20), *Desulfobacterium niacini* (S-G-Dsbm-0804-a-A-18), and *Methanogenium cariaci* JR1 (= DSM 1497) (S-O-Mmic-1200-a-A-21) (1, 8, 21, 25, 26, 31).

Nucleotide sequence accession numbers. The partial SSU rRNA gene sequences determined in this study have been deposited in the GenBank database under accession numbers AF218215 through AF218222.

RESULTS AND DISCUSSION

Preperturbation community structure. Both the HS and LS sets of reactors performed uniformly before the glucose shock, indicating a replication of function (11). Immediately before the glucose shock (day 0), microbial community structure and the extent of community replication were evaluated by morphological analysis, ARDRA, and SSU rRNA oligonucleotide probing. Morphological analysis targeted the entire microbial diversity present at an abundance of ≥0.1%, while ARDRA targeted the major bacterial populations only. Methanogens and less predominant functional groups within the *Bacteria*, such as syntrophic organisms and SRB, were evaluated with SSU rRNA oligonucleotide probes.

(i) Morphological analysis. The eight reactors segregated according to origin into two major types of communities before the glucose perturbation (Fig. 1). One community type, represented by reactors 5 through 8, had 11 recognizable OMUs and was dominated numerically by spirals and short, straight, F_{420} autofluorescent rods (Fig. 1 and 2). The other community type, exemplified by reactors 1 through 4, had 14 recognizable OMUs and was dominated by cocci occurring singly and in clusters (Fig. 1). Reactors 1 through 4 also had low frequencies of spiral and other unique morphotypes (e.g., coiled filaments, rods and cocci in chains, rods with irregular axes, ovoids with refractile lines, and prosthecates). Based on these morphological distinctions, reactors 5 through 8 were designated HS communities and reactors 1 through 4 were designated LS communities. The only cell morphotype that could not be included in this quantitative assessment of morphological diversity was the pseudosarcina morphotype, because most of these cells remained tightly packed into three-dimensional aggregates after specimen preparation (Fig. 2A). These aggregates

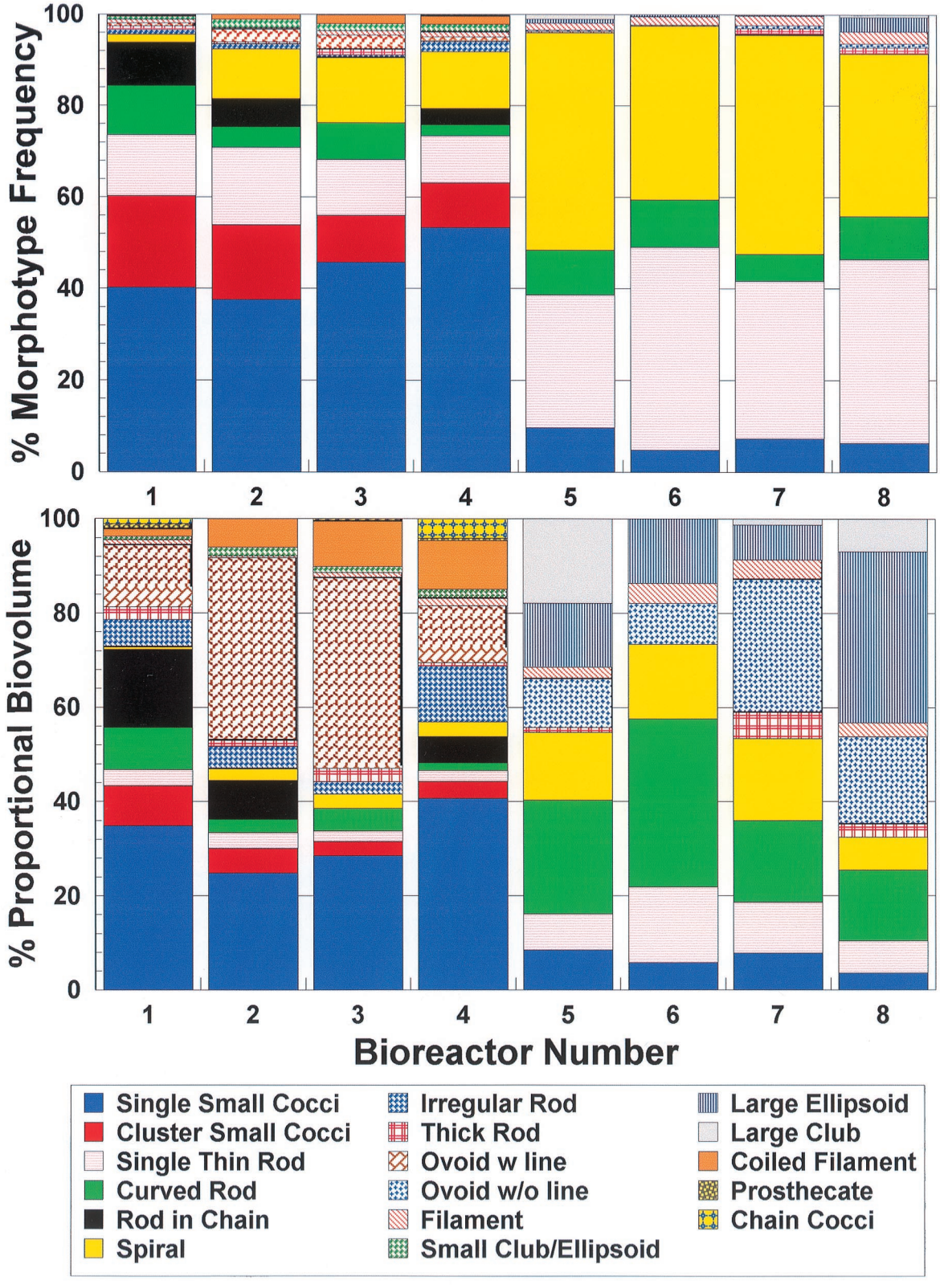

FIG. 1. Replication of preperturbation community structure in the eight bioreactors: community morphotype frequency and proportional biovolume calculated by computer-assisted microscopy and image analysis. Some of the single thin rods exhibited autofluorescence emission at 420 nm. The LS reactors were reactors 1 through 4, and the HS reactors were reactors 5 through 8.

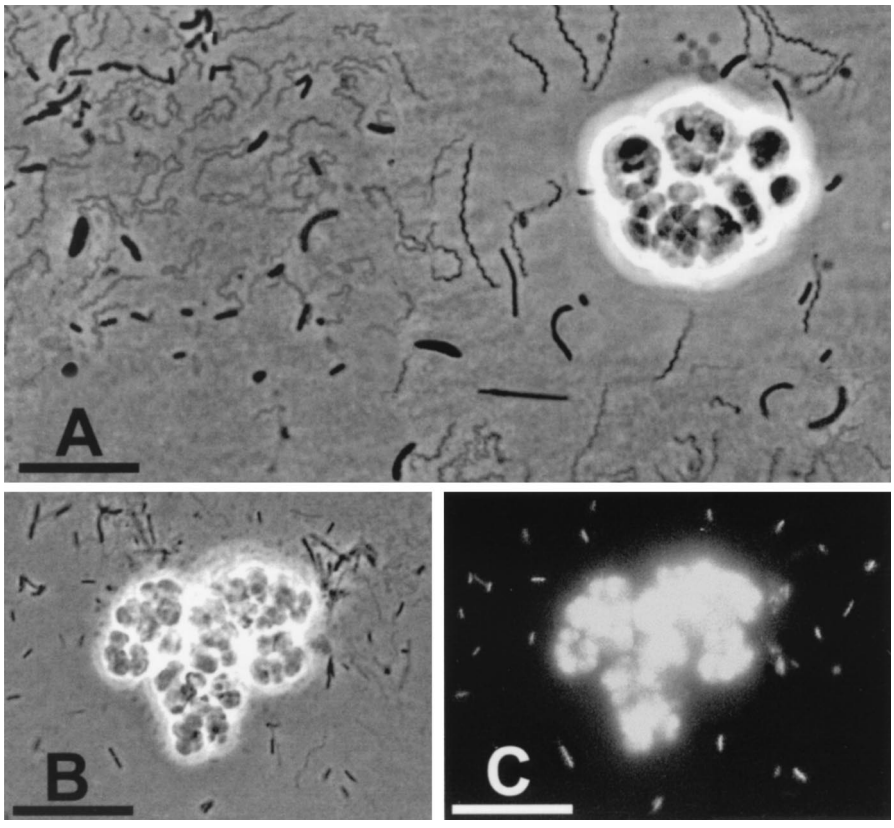

FIG. 2. Micrographs of community samples from the HS reactor set. (A) Phase-contrast micrograph showing various distinct morphotypes, including spirals, short straight rods, curved rods, thin filaments, thick rods, single cocci, and an aggregate of pseudosarcina units. (B and C) Phase-contrast micrograph (B) and epifluorescence micrograph (C) of the same field of view, indicating that the aggregated pseudosarcina units and single short straight rods exhibit F_{420} autofluorescence. Bars = 10 μm.

occurred in 5% of the phase-contrast micrographs of the HS reactor samples and in none of the LS reactor samples.

Computation of biovolumes significantly altered the picture of community structure for all bioreactors, with greater recognition of the significant biomass contributed by less frequent morphotypes to community structure (Fig. 1). Although the smaller morphotypes occurred more frequently than the larger morphotypes, the larger biovolumes of the some of the rare morphotypes made their contributions to the community structure significant. This is further demonstrated by comparison of the J evenness community index (H'/H'_{max}) for all eight bioreactors when either proportional biovolume or morphotype frequency is used. The evenness in distribution of morphotypes for all eight reactors was higher when it was based on biovolumes (mean J = 0.81) than when it was based on frequencies (mean J = 0.65). The mean biovolume per cell for the 18 different morphotypes (in cubic micrometers per cell; $n = 100$ cells/morphotype) varied considerably, as follows: short thin rods, 0.3; spirals, 0.4; small cocci in clusters, 0.5; single small cocci, 1.1; small clubs, 1.6; straight filaments, 2.0; rods in chains, 2.2; curved rods, 2.7; pseudosarcinae, 4.1; large thick rods, 4.2; irregular rods, 7.6; coiled filaments, 8.4; prosthecates, 9.2; large cocci in chains, 19.0; large clubs, 20.9; ellipsoids, 21.9; ovoids with a refractile line, 22.5; and ovoids without a refractile line, 42.1.

Morphotype diversity calculated as Shannon-Weiner indices based on morphotype frequency showed that the LS set was more diverse ($H' = 1.72 \pm 0.18$) than the HS set ($H' = 1.33 \pm 0.22$) before the perturbation. The Mann-Witney test statistic indicated that these mean H′ values differ at the 95% confidence level ($P = 0.0304$).

(ii) ARDRA. The bacterial component of microbial community structure was successfully replicated at the ribotype level in the HS set but was only partially replicated in the LS set. As shown in Fig. 3B, two OTUs—HS I and HS II—dominated all four HS communities (reactors 5 through 8). Partial sequences for HS I and HS II were identical and clustered with *Spirochaeta caldaria* and other freshwater spirochetes (Fig. 4). These data suggest that the bacterial component of the HS communities was dominated by spirochetes. This is consistent with the prevalence of spiral cells in the morphotype analysis and confirms that the large number of *Spirochaeta*-related clones obtained was not a PCR or cloning artifact. The other numerically dominant morphotype in the HS communities, short straight rods, was F_{420} autofluorescent (Fig. 1 and 2), indicating that this morphotype was a methanogen that would not be detected in the *Bacteria*-specific ARDRA.

Community structure was not as well replicated for the LS reactor set at the ribotype level (Fig. 3B). This was indicated by variability in the frequency of the dominant OTUs (LS I, LS II, and LS III). None of these OTUs was detected in all four reactors. The distribution of OTUs demonstrated that the LS set contained two community types. Reactors 1 and 3 were dominated by LS II and LS III, while reactors 2 and 4 were more diverse and LS I was the dominant ribotype. The partial sequence LS I clustered within a deeply branching group of the order *Spirochaetales* that contains free-living, wall-less strains reported to exhibit pleomorphic coccus and budding morphol-

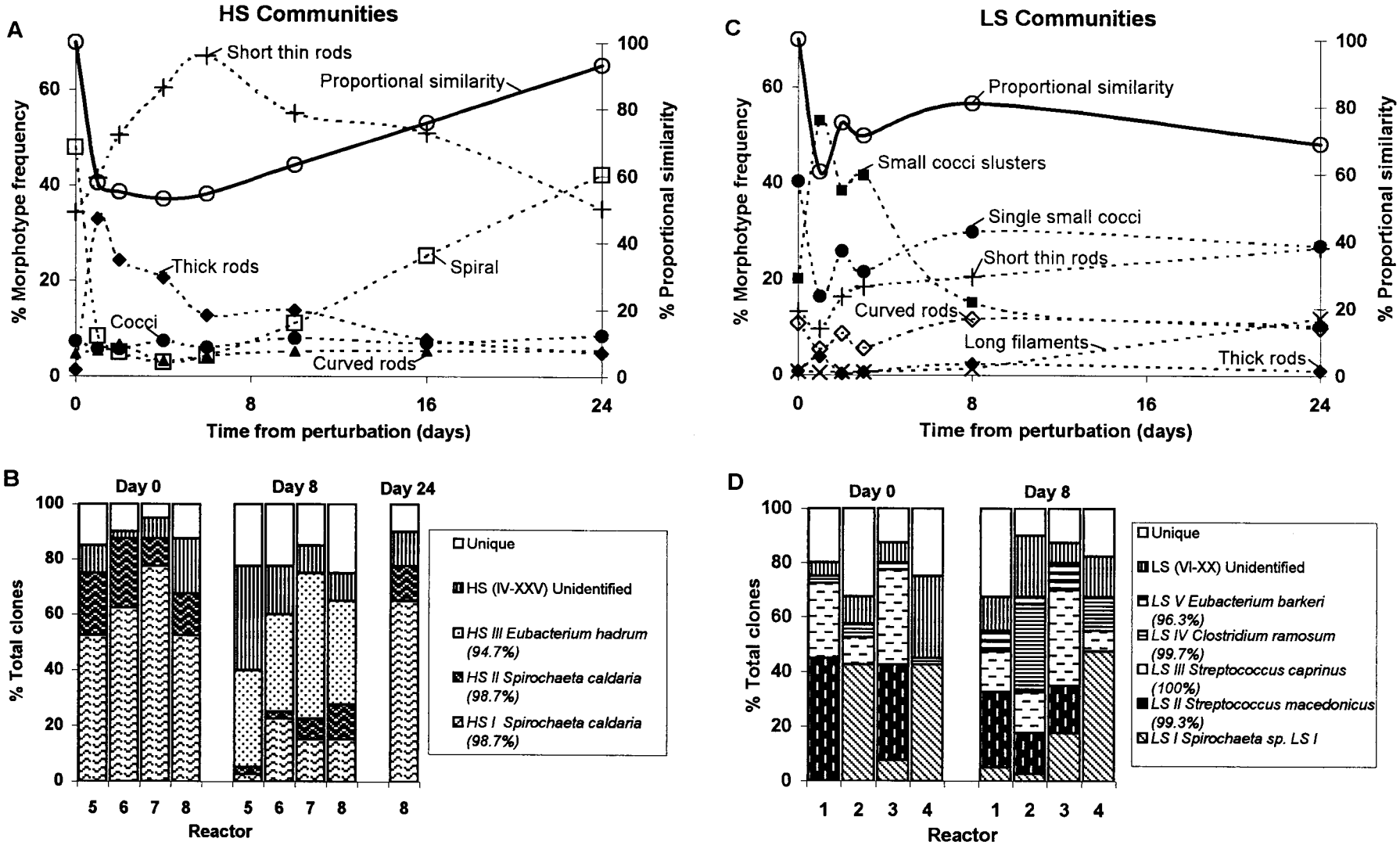

FIG. 3. Responses of the HS (A and B) and LS (C and D) communities to the glucose perturbation. (A and C) Morphotype frequency and proportional community similarity in reactor 7 (A) and reactor 1 (C). (B and D) ARDRA of the reactor communities 0, 8, and 24 days after the perturbation. Only reactor 8 was analyzed on day 24. Unique OTUs were defined as those that occurred once in each clone library (e.g., they were observed only once throughout the entire study in each reactor set). Species names indicate the most closely related known organisms. Percent similarities are indicated in parentheses.

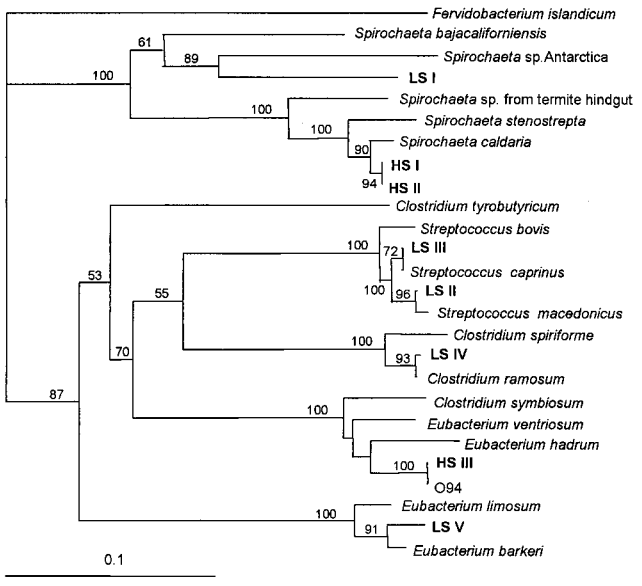

FIG. 4. Phylogram of the dominant SSU rDNA clones from the HS and LS communities created from analysis of 330 nucleotides of the 16S rRNA gene corresponding to positions 121 to 451 of *Escherichia coli*. Bootstrap values from 100 replicates are shown for each node. Values less than 50 are not shown. The scale bar represents a 10% estimated difference in nucleotide sequence. Clones obtained from the reactors are in boldface. The EMBL accession number for the *Spirochaeta* sp. from termite hindgut is X89048.

ogies rather than spirals (7); however, the closest known relative of LS I had only 81.1% sequence similarity (Fig. 4). LS II and LS III were closely related to each other (98.4% sequence similarity) but were only distantly related to LS I. LS II was 99.3% similar to *Streptococcus macedonicus*, and LS III was 100% similar to *Streptococcus caprinus* (Fig. 4).

The dominant bacterial ribotypes reflected the dominant morphotypes for LS reactors 1 and 3 but not for LS reactors 2 and 4. The dominant coccal morphotype in reactors 1 and 3 is consistent with the *Streptococcus*-related ribotypes in these reactors, but the spiral shape expected for the dominant *Bacteria* ribotype (LS I) in reactors 2 and 4 was infrequent (Fig. 1). However, despite the fact that dominant *Bacteria* ribotype LS I in reactors 2 and 4 was distantly related to other *Spirochaeta* SSU rRNA sequences, spiral morphotypes occurred in these bioreactors at relative frequencies of only 10.9 and 12.4%, respectively (Fig. 1). In light of the fact that LS I's closest known relative, *Spirochaeta* sp. strain Antarctic, lacks the expected spiral shape of all other spirochetes (7), the dominant spirochete-related LS I ribotype in reactors 2 and 4 does not exhibit a spiral shape but instead is classified as another morphotype (possibly single cocci) by microscopic analysis. This serves as a clear example of how morphological and ribotype analyses can work together to reveal features of microbial community structure that otherwise remain obscure when either approach is used alone.

Before the perturbation, the HS set was uniformly dominated by spirochetes while the LS set was more variable, with a greater contribution from infrequent and unique OTUs (Fig. 1 and 3B). Shannon's diversity index based on OTU frequency illustrates that the LS set was more diverse ($H' = 2.01 \pm 0.31$) than the HS set ($H' = 1.32 \pm 0.41$). Although neither ARDRA nor morphological analysis may be capable of detecting all of the diversity present in a complex microbial community, both methods indicated that the LS set was more diverse than the HS set. This difference in diversity may have been caused by the history of the inoculum used for each set of reactors. Inoculum for the HS set was obtained from a 16-liter bioreactor that had operated for 200 days (12.5 mean cell residence times) with glucose as the sole carbon and energy source, whereas inoculum for the LS set was obtained from a 16-liter bioreactor that had been supplied with glucose for only 60 days (3.75 mean cell residence times). Thus, although both 16-liter reactors were inoculated with anaerobic digestor sludge from the same wastewater treatment plant, the LS reactor set received less extensive selection on glucose, possibly resulting in a more diverse community on day 0.

(iii) Methanogens, SRB, and syntrophs. Two reactors from each set of replicates were chosen for rRNA membrane hybridization analysis: reactors 6 and 7 from the HS set and reactors 1 and 2 from the LS set. Replicate communities were similar for each set of reactors, but the HS and LS sets differed significantly on day 0 (Fig. 5). In the HS set, the *Methanosarcina*-specific probe S-G-Msar-0821-a-A-24 accounted for 63% ± 1% (reactor 6) and 61% ± 1% (reactor 7) of the rRNA detected by all of the methanogen-specific probes used. The *Methanosaeta*-specific probe S-G-Msae-0381-a-A-22 accounted for 19% ± 4% (reactor 6) and 11% ± 5% (reactor 7). In contrast, in the LS set the *Methanosarcina*-specific probe detected only 1% ± 0.3% of the rRNA detected by all of the methanogen-specific probes, while the *Methanosaeta*-specific probe detected up to 38% (Fig. 5). Additional differences were found among CO_2-reducing methanogenic genera. Species belonging to the families *Methanomicrobiaceae*, *Methanocorpusculaceae*, and *Methanoplanaceae* detected with probe S-O-Mmic-12000-a-A-21 accounted for over 60% of the methanogen-specific probes in the LS set and less than 20% in the HS set. Lastly, the specific probe for the order *Methanobacteriales* detected between 6 and 12% of the methanogen rRNA in the HS set and between 0 and 1% of the methanogen rRNA in the LS set (Fig. 5). There may have been other methanogens present that were not detected by the methanogen-specific probes used in this study; however, previous studies have found that these probes detect the majority of methanogens present in mesophilic sewage sludge digesters (8, 21).

Combined phase-contrast and epifluorescence microscopy (365-nm excitation, 420-nm emission) revealed three different autofluorescent morphotypes in all four reactors of the HS set:

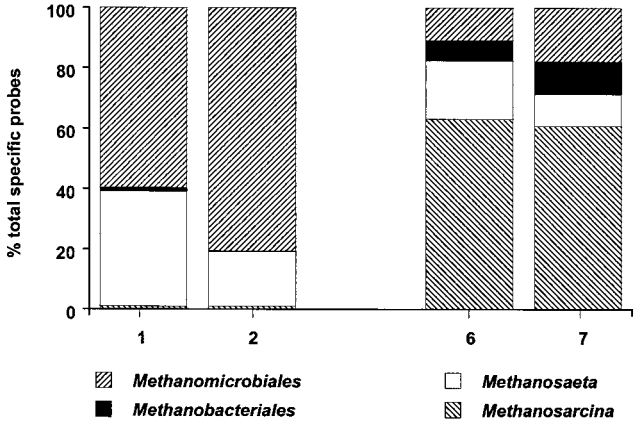

FIG. 5. Relative abundances of methanogen-related SSU rRNA in LS reactors 1 and 2 and HS reactors 6 and 7 on day 0 determined by SSU rRNA membrane hybridization to oligonucleotide probes. The abundance of each group is expressed as a percentage of the total amount of methanogen-related SSU rRNA detected by all of the methanogen-specific probes used.

(i) short, thin, straight rods; (ii) thicker, longer rods with an irregular axis; and (iii) aggregates of closely associated pseudosarcina units resembling *Methanosarcina* species cells (29) (Fig. 2). The latter aggregates were various sizes and occurred at a frequency of one aggregate per 20 microscopic fields of view. Several morphotypes of F_{420} fluorescent cells were present in the LS communities; these morphotypes included short thin rods, rods in chains, cocci, and ovoids with a refractile line. Aggregates of autofluorescent cells resembling *Methanosarcina* species cells were not observed in the LS communities, which is consistent with the very small amount of *Methanosarcina*-related SSU rRNA detected in reactors 1 and 2.

Syntrophic propionate and butyrate oxidizer rRNA was detected at low levels in all of the reactors sampled. The levels varied between 2 and 4% of the rRNA detected with general bacterial probe S-D-Bact-0338-a-A-18 (data not shown). SRB-related rRNA was present in both sets of reactors at levels between 6 and 15% of the *Bacteria* rRNA. *Desulfovibrio*-related rRNA (S-F-Dsv-0687-a-A-16) was the most abundant rRNA in all reactors (the signals were 5 to 6 times greater than the signals with probes S-G-Dsbm-0804-a-A-18 and S-G-Dsbb-0660-a-A-20) (data not shown). No significant differences were detected between the two sets of reactors for any of the syntrophic bacterium- or SRB-targeted probes.

(iv) Summary. All eight reactors performed uniformly for 2 weeks before the disturbance (11), indicating that there was replication of function without replication of community structure. We have previously described a similar situation for a glucose-fed bioreactor that experienced a shift in community structure with no detectable change in performance (6). In general, the two sets of bioreactor communities had very different fermentative and methanogenic populations, with the HS set being less diverse and better replicated.

Perturbation response. Following the glucose perturbation, two reactors in the HS set (reactors 6 and 7) and two reactors in the LS set (reactors 1 and 4) were periodically monitored by morphological analysis. In addition, all eight reactors were periodically monitored for changes in bacterial community structure by ARDRA (Fig. 3).

(i) HS reactor set. In the HS set, the added glucose was simultaneously converted to butyrate and acetate, and minor proportions of lactate and propionate were also produced. The same fermentation pattern was observed in all four reactors (11). Conversion of the added glucose was accompanied by a rapid decrease in the proportion of *Spirochaeta*-related rDNA clones and spiral morphotypes, a dramatic increase in the proportion of *Eubacterium*-related rDNA OTUs and thick rods, and an increase in the proportion of short thin rods (Fig. 3A and B). Shannon's diversity index based on OTU frequency (H′) also increased from 1.32 ± 0.41 before the perturbation to 2.13 ± 0.33 on day 8 after the perturbation.

Spirochetes evidently played a significant role in the preperturbation community but were less important in the fermentation of the spike of added glucose. Members of the genus *Spirochaeta* generally ferment glucose directly to acetate and small amounts of ethanol and lactate (3, 17). This fermentation pattern was found in a spiral bacterium recently isolated from a similar glucose-fed methanogenic reactor (data not shown). Many spirochetes are also slowly growing organisms (3, 10), and the initial slow rate of glucose utilization observed is consistent with this (11).

The dominant OTU following the perturbation (HS III) was not detected by ARDRA in any of the HS reactors on day 0, but on day 8 it dominated all HS reactors (Fig. 3B). We previously isolated a rod-shaped bacterium with an identical sequence, strain O94, from a similar methanogenic reactor fed discontinuously with glucose (6) (Fig. 4). The fermentation products of strain O94 are mainly butyrate and acetate (data not shown), suggesting that HS III was responsible for the accumulation of these products. This metabolism was important in the fermentation of the excess glucose in the HS reactors, with over 30% of the electron equivalents from glucose converted to butyrate (11). Morphological analysis of reactors 6 and 7 supported the ARDRA data and allowed rapid assessment of the change in community structure at frequent intervals after the glucose perturbation, which was not possible with ARDRA. A rapid and transient increase in the proportion of thick rods was highly correlated with the appearance of butyrate in the reactor (Fig. 3A) (11). These rods were very similar in appearance to strain 094 cells and eventually produced refractile endospores (data not shown). Although fluorescent in situ hybridization was not performed, morphological analysis gave quantitative results that confirmed the results of ARDRA, which is more qualitative and subject to a number of biases (25, 31).

Both morphological and rDNA analyses indicated that the HS reactor communities recovered between 16 and 24 days after the glucose shock. The proportional community similarity index based on a comparison of morphotype frequencies in communities sampled at time t_x relative to the frequencies at time zero decreased 53% after the perturbation and then increased steadily to 90% by day 24 in reactor 7 (Fig. 3A). A similar dramatic decline occurred in HS reactor 6, and there was a return to 93% proportional similarity by day 16 (data not shown). Spiral-shaped organisms and thick rods also returned to their preperturbation frequency by this time. In addition, the proportions of the spirochete-related OTUs HS I and HS II increased between day 8 and day 16 (data not shown). By day 24, ARDRA analysis of reactor 8 indicated that HS I and HS II accounted for 78% of the 40 clones analyzed, compared to 70% on day 0 (Fig. 3B). Functional parameters also returned to the preperturbation state (11).

(ii) LS reactor set. A distinctly different response was observed in the LS reactor set. For three of the four reactors, glucose was first fermented to lactate and then converted to butyrate and finally to acetate. Propionate appeared later but was present at low concentrations (11). In reactors 1 through 3, *Streptococcus*- and *Clostridium*-related OTUs were predominant following the glucose shock. The proportions of unique OTUs and low-frequency morphotypes also increased (Fig. 3C and D). An increase in the proportion of minor morphotypes and OTU diversity suggests that many *Bacteria* and *Archaea* populations were favored by the glucose shock but that none of these populations displaced the initially dominant populations except in reactor 2. The fourth reactor, which behaved differently in function (11), underwent only small community changes after the perturbation (Fig. 3D).

Despite the variation observed in the LS set, similarities among reactors 1 through 3 were discernible. *Streptococcus*-related OTUs (LS II and LS III) and coccal morphotypes remained prevalent in reactors 1 and 3 and their proportions increased in reactor 2, indicating that *Streptococcus*-like bacteria were responsible for the rapid accumulation of lactate in reactors 1, 2, and 3 (30) (Fig. 3C and D). The simultaneous degradation of lactate and accumulation of butyrate in these three reactors suggest that lactate was reduced to butyrate (11). Many low-G+C-content gram-positive organisms, such as *Butyrivibrio methylotrophicum* and *Clostridium butyricum*, are capable of fermenting lactate to butyrate (2, 23). The proportions of OTUs related to *Clostridium ramosum* (LS IV) and *Eubacterium barkeri* (LS V) increased in reactors 1 through 3 between day 0 and day 8. The prevalence of LS IV and LS V

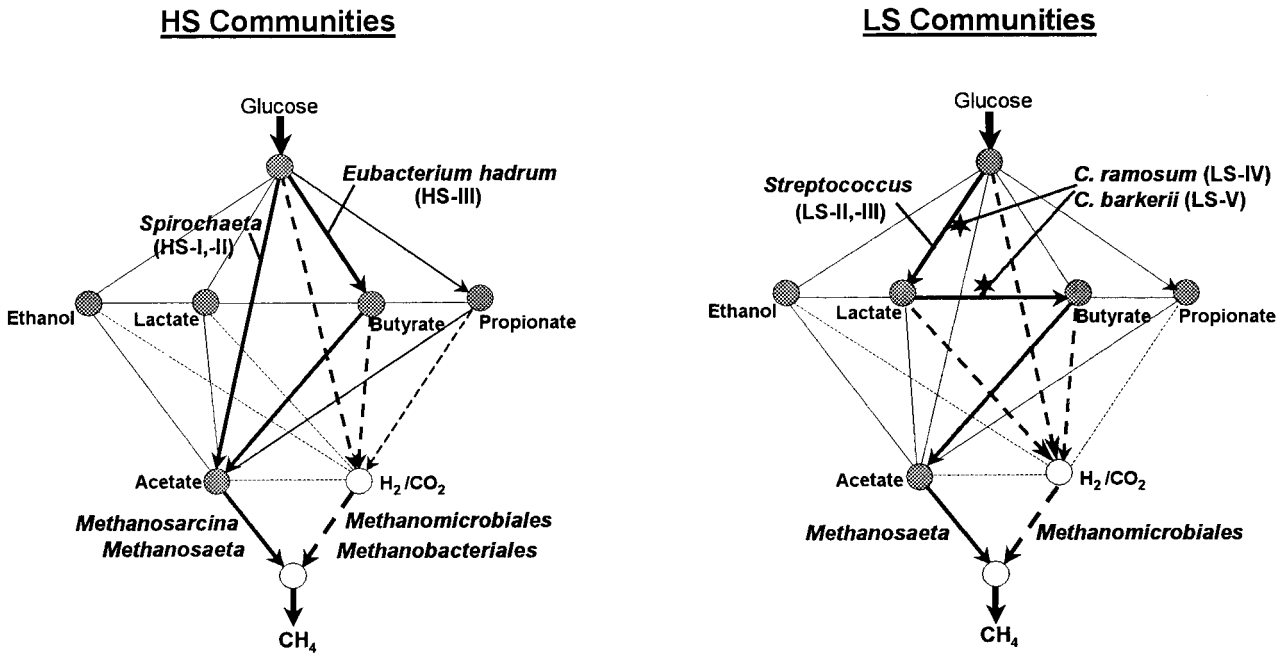

FIG. 6. Network model of community structure and function in the HS and LS bioreactors during the glucose perturbation. The dotted lines and open circles indicate gas products. The thickness of each line represents the relative contribution of the pathway. The stars indicate in situ activities whose assignments to specific organisms are highly questionable due to the metabolic diversity of the most similar cultured organisms.

varied in reactors 1, 2, and 3, with LS IV being very dominant in reactor 2 and absent from reactors 1 and 3 (Fig. 3D). *E. barkeri* and *C. ramosum* have different physiologies, but both are saccharolytic specialists capable of fermenting glucose to different ratios of butyrate, lactate, and acetate and different ratios of formate, acetate, and lactate, respectively. The appearance of ribotypes LS IV and LS V in the LS set suggests that the corresponding organisms may have played a role in the carbon conversions that occurred after the accumulation of lactate. However, they could also have fermented glucose, and further experimentation is needed to determine if the organisms represented by LS IV and LS V ferment lactate to butyrate.

Morphological analysis of reactor 1 revealed a significant increase in the frequency of minor morphotypes after the perturbation, which was reflected in an increase in diversity from $H' = 1.71$ on day 0 to $H' = 2.12$ on day 8 and $H' = 2.23$ on day 24. This is consistent with the average increase in ARDRA OTU diversity from $H' = 2.01 \pm 0.31$ on day 0 to $H' = 2.18 \pm 0.31$ on day 8. Changes in the frequency of cocci directly after the perturbation and long-term increases in the frequencies of several other morphologies, such as short thin rods, curved rods, prosthecates, and unbranched filaments, significantly changed the community structure, as indicated by a decrease in the proportional community similarity index to 60% (Fig. 3C). However, this change was less pronounced than the community shift that occurred after the perturbation in the HS set and did not involve the displacement of the most dominant organisms (Fig. 3). The LS bacterial community was therefore more stable and less flexible than the HS community because the main fermenting populations were not displaced during the perturbation as they were in the HS community. In contrast to the community behavior, the HS reactors were more functionally stable following the glucose shock (11).

Despite similarities in initial community structure between reactors 2 and 4 (Fig. 1 and 3), the response of reactor 4 to the glucose shock was unique. Functionally, this reactor accumulated large amounts of ethanol and was the least stable of the eight reactors analyzed (11). The frequency of the most prevalent bacterial ribotype—*Spirochaeta* sp. LS I—remained unchanged and *Streptococcus*- and *Clostridium*-related ribotypes became detectable following the perturbation (Fig. 3D). Morphological analysis of this reactor 24 h after the glucose shock revealed that the proportions of all dominant morphotypes remained the same (data not shown). Changes in community composition that occurred in reactor 2 correlated with more functional stability following the substrate perturbation, while the structural stability of the reactor 4 community corresponded with poor functional stability.

Although there were many significant changes in the LS communities after the perturbation, the dominant fermenting bacteria before the perturbation were responsible for fermentation of the added glucose in the LS reactors, while in the HS communities an undetected population rapidly arose and fermented the excess glucose; therefore, the HS community structure was less stable than the LS community structure during this perturbation. This implies that functional stability does not necessarily correlate with stability in community structure and even suggests that a less flexible or more "stable" microbial community structure results in poor function following a significant perturbation. This may be because organisms that are dominant under steady-state conditions are not the organisms best adapted to perturbed conditions. Although the perturbation affected the HS communities more than the LS communities, the HS communities recovered to their preperturbation state within 16 days. Thus, the perturbation did not permanently alter the entire HS community structure even though minority community members responded to the perturbation, again demonstrating the flexibility of this community.

Community model and implications. The polyphasic approach of combining several methods (morphological analysis, ARDRA, SSU rRNA probes, and functional analysis) used in

this study and in a companion study (11) allowed us to overcome methodological limitations and develop a network model of community structure and function based on the anaerobic food chain (Fig. 6). The large population of spirochetes in the HS community mainly fermented glucose under preperturbation conditions. When a large pulse of glucose was applied, the fast-growing organism *Eubacterium* sp. strain O94 that was initially present at very low levels emerged and outcompeted the more slowly growing spirochete population, eventually shifting 30% of the electron and carbon flow through butyrate. The high proportion of fast-growing acetoclastic *Methanosarcina* species in these reactors rapidly metabolized acetate generated after the perturbation, resulting in little accumulation of acetate (29). It is important to note that even though we used a number of community analysis techniques, we were unable to define the populations responsible for every metabolic activity in the HS community, such as the conversion of glucose to propionate or the conversion of butyrate to acetate.

A unifying model of community structure and function for the LS reactors is less clear because of the greater variability in the community structure of these reactors. The greater variability and diversity in the LS communities may be a result of the reduced amount of time that this set of bioreactors was operated in the laboratory. It might be expected that the greater diversity of these communities would result in a better functional response to a perturbation, but we found that this was not the case. In reactors 1, 2, and 3 it appears that *Streptococcus*-like organisms rapidly produced large amounts of lactate during the glucose shock. Streptococci typically have high growth rates (30), which probably allowed them to remain predominant following the substrate shock. Lactate was then converted to butyrate by other fermentative bacteria. Only low-G+C-content gram-positive bacteria have been reported to convert lactate to butyrate, implying that perhaps the *Clostridium*-related species that became abundant after the perturbation performed this conversion; however, clostridia have a broad metabolic potential and the in situ activity of uncultured populations is difficult to infer from only phylogenetic information. Conversion of butyrate to acetate by an undefined population resulted in accumulation of acetate (11). This was likely due to the predominance of slowly growing acetoclastic *Methanosaeta* species. The carbon conversions that took place in the LS reactors were serial in nature, in contrast to the parallel conversions in the HS reactors, and may have contributed to the functional instability of the LS reactors (11) (Fig. 6).

Despite the differences in the HS and LS communities, the relative frequencies of ribotypes belonging to the *Eubacterium-Clostridium* group increased after the glucose shock in all eight reactors (Fig. 3B and D). Although these ribotypes were not closely related phylogenetically, they all likely had the ability to produce large amounts of H_2, shifting the reducing equivalents directly to a neutral, methanogenic substrate that was rapidly utilized and possibly conferring functional stability on the ecosystem (15). In both types of reactors there was also an increase in ribotype and morphotype diversity after the perturbation, demonstrating that fluctuating environmental conditions can indeed increase the diversity of microbial communities. In addition, replication of the HS response indicates that although undetectable members may play an important role in a perturbation response, their response is not stochastic and thus may be predicted. These results also show that mathematical models based exclusively on dominant populations have limited predictive power.

Conclusions. This study demonstrates that some reproducibility in community structure and response is feasible for complex bioreactor communities, and hence it should facilitate the use of bioreactors in the study of ecological questions. Syntrophs and other minority populations represent a significant uncertainty in this system because they are present at relatively low levels yet have a critical functional role; however, our results indicate that the impact of minority members is reproducible and thus should be included in mathematical models of bioreactor communities.

An important issue in the management of complex ecosystems is how functional stability relates to population stability and diversity. Functional stability could not be attributed to higher species diversity or community stability in this study. The glucose shock altered the *Bacteria* composition of the HS reactors more profoundly than that of the LS reactors, yet the HS reactors were functionally more stable. In addition, different biochemical pathways were active in the two reactor sets, possibly affecting the functional stability (11). These results indicate that stability is linked to community flexibility reflected in the ability to shift the electron and carbon flow through various alternative guilds in an efficient manner.

ACKNOWLEDGMENTS

This research was supported by NSF grant DEB 9120006 to the Center for Microbial Ecology. A.S.F. was partially supported by an OAS grant and by the Comisión Secretorial de Investigación Científica, Universidad de la República, Montevideo, Uruguay.

We are grateful to Kay Gross (Kellogg Biological Station, Michigan State University) for her valuable discussions about ecological concepts throughout the course of this work and to Suiying Huang for her help with the ARDRA.

REFERENCES

1. **Amann, R. I., B. J. Binder, R. J. Olson, S. W. Chrisholm, R. Devereux, and D. A. Stahl.** 1990. Combination of SSU rRNA-targeted oligonucleotide probes with flow cytometry for analyzing mixed microbial populations. Appl. Environ. Microbiol. **56:**1919–1925.
2. **Brauman, A., S. Keleke, M. Malonga, E. Miambi, and F. Ampe.** 1996. Microbiological and biochemical characterization of cassava retting, a traditional lactic acid fermentation for foo-foo (cassava flour) production. Appl. Environ. Microbiol. **62:**2854–2858.
3. **Canale-Parola, E.** 1977. Physiology and evolution of spirochetes. Bacteriol. Rev. **41:**181–204.
4. **Dazzo, F. B., and M. Petersen.** 1989. Applications of computer-assisted image analysis for microscopical studies of the *Rhizobium*-legume symbiosis. Symbiosis **7:**193–210.
5. **Felsenstein, J.** 1985. Confidence limits of phylogenies: an approach using the bootstrap. Evolution **39:**783–791.
6. **Fernandez, A., S. Huang, S. Seston, J. Xing, R. F. Hickey, C. Criddle, and J. Tiedje.** 1999. How stable is stable? Function versus community stability. Appl. Environ. Microbiol. **65:**3697–3704.
7. **Franzman, P. D., and S. J. Dobson.** 1992. Cell wall-less, free-living spirochetes in Antarctica. FEMS Microbiol. Lett. **97:**289–292.
8. **Hansen, K. H., B. K. Ahring, and L. Raskin.** 1999. Quantification of syntrophic fatty acid-β-oxidizing bacteria in a mesophilic biogas reactor by oligonucleotide probe hybridization. Appl. Environ. Microbiol. **65:**4767–4774.
9. **Harmsen, H. J. M., H. M. P. Kengen, A. D. L. Akkermans, A. J. M. Stams, and W. M. de Vos.** 1996. Detection and localization of syntrophic propionate-oxidizing bacteria in granular sludge by in situ hybridization using rRNA-based oligonucleotide probes. Appl. Environ. Microbiol. **62:**1656–1663.
10. **Harwood, C. S., and E. Canale-Parola.** 1983. *Spirochaeta isovalerica* sp. nov., a marine anaerobe that forms branched-chain fatty acids as fermentation products. Int. J. Syst. Bacteriol. **33:**573–579.
11. **Hashsham, S. A., A. S. Fernandez, S. L. Dollhopf, F. B. Dazzo, R. F. Hickey, J. M. Tiedje, and C. S. Criddle.** 2000. Parallel processing of substrate correlates with greater functional stability in methanogenic bioreactor communities perturbed by glucose. Appl. Environ. Microbiol. **66:**4050–4057.
12. **Liu, J., F. B. Dazzo, O. Glagoleva, B. Yu, and A. Jain.** CMEIAS©: a computer-aided system for the image analysis of bacterial morphotypes in microbial communities. Microb. Ecol., in press.
13. **Massol-Deya, A. A., D. A. Odelson, R. F. Hickey, and J. M. Tiedje.** 1995. Bacterial community fingerprinting of amplified SSU and 16-23S ribosomal DNA gene sequences and restriction endonuclease analysis (ARDRA), p. 3.3.2:1–3.3.2:8. *In* A. D. L. Akkermans, J. D. Van Elsas, and F. J. de Bruijn (ed.), Molecular microbial ecology manual. Kluwer Academic Publishers, Dordrecht, The Netherlands.

14. **McCarty, P. L., and F. E. Mosey.** 1991. Modeling of anaerobic digestion processes (a discussion of concepts). Water Sci. Technol. **24:**17–33.
15. **Mosey, F. E., and X. A. Fernandes.** 1989. Patterns of hydrogen in biogas from the anaerobic digestion of milk-sugars. Water Sci. Technol. **21:**187–196.
16. **Pfennig, N., and S. Wagener.** 1986. An improved method of preparing wet mounts for photomicrographs of microorganisms. J. Microbiol. Methods **4:**303–306.
17. **Pohlschroeder, M., S. B. Leschine, and E. Canale-Parola.** 1994. *Spirochaeta caldaria* sp. nov., a thermophilic bacterium that enhances cellulose degradation by *Clostridium thermocellum*. Arch. Microbiol. **161:**17–24.
18. **R & M Biometrics.** 1990. Bioquant Image Analysis software. R & M Biometrics, Nashville, Tenn.
19. **Raskin, L., L. K. Poulsen, D. R. Noguera, B. E. Rittmann, and D. A. Stahl.** 1994. Quantification of methanogenic groups in anaerobic biological reactors by oligonucleotide probe hybridization. Appl. Environ. Microbiol. **60:** 1241–1248.
20. **Raskin, L., B. E. Rittmann, and D. A. Stahl.** 1996. Competition and coexistence of sulfate-reducing and methanogenic populations in anaerobic biofilms. Appl. Environ. Microbiol. **62:**3847–3857.
21. **Raskin, L., J. M. Stromley, B. E. Rittmann, and D. A. Stahl.** 1994. Group-specific rRNA hybridization probes to describe natural communities of methanogens. Appl. Environ. Microbiol. **60:**1232–1240.
22. **Saitou, N., and M. Nei.** 1989. The neighbor-joining method: a new method of reconstructing phylogenetic trees. Mol. Biol. Evol. **4:**406–425.
23. **Shen, J. G., B. A. Annous, R. W. Lovitt, M. K. Jain, and J. G. Zeikus.** 1996. Biochemical route and control of butyrate synthesis in *Butyribacterium methylotrophicum*. Appl. Microbiol. Biotechnol. **45:**355–362.
24. **Smith, D. P., and P. L. McCarty.** 1990. Factors governing methane fluctuations following shock loading of digesters. J. Water Pollut. Control Fed. **62:**58–64.
25. **Snaidr, J., R. Amann, I. Huber, W. Ludwig, and K. H. Schleifer.** 1997. Phylogenetic analysis and in situ identification of bacteria in activated sludge. Appl. Environ. Microbiol. **63:**2884–2896.
26. **Stahl, D. A., B. Flesher, H. R. Mansfield, and L. Montgomery.** 1988. Use of phylogenetically based hybridization probes for studies of ruminal microbial ecology. Appl. Environ. Microbiol. **54:**1079–1084.
27. **Tchobanoglous, G., and F. L. Burton.** 1991. Wastewater engineering: treatment, disposal, and reuse, 3rd ed. Irwin McGraw Hill, Inc., New York, N.Y.
28. **Thompson, J. D., D. G. Higgins, and T. J. Gibson.** 1994. CLUSTAL W: improving the sensitivity of progressive multiple sequence alignment through sequence weighting, position-specific gap penalties and weight matrix choice. Nucleic Acids Res. **22:**4673–4680.
29. **Whitman, W. B., T. L. Bowen, and D. R. Boone.** 1992. The methanogenic bacteria, p. 719–767. *In* A. Balows, H. G. Trüper, M. Dworkin, and K. H. Schleifer (ed.), The prokaryotes. A handbook on the biology of bacteria: ecophysiology, isolation, identification, applications, 2nd ed. Springer-Verlag, New York, N.Y.
30. **Yamada, T., and J. Carlsson.** 1975. Regulation of lactate dehydrogenase and change of fermentation products in streptococci. J. Bacteriol. **124:**55–61.
31. **Zheng, D., E. W. Alm, D. A. Stahl, and L. Raskin.** 1996. Characterization of universal small-subunit rRNA hybridization probes for quantitative molecular microbial ecology studies. Appl. Environ. Microbiol. **62:**4504–4513.